

Electronic Supplementary Information

Ratiometric Detection of HSA Using Aggregation Induced Enhanced Emission Conjugated Polyelectrolyte and Prototype Smartphone Device

Moirangthem Anita Chanu,^a Dheeraj Dineshbhai Khubchandani,^a Laxmi Raman Adil,^a Priyam Ghosh,^a and Parameswar Krishnan Iyer^{*a,b,c}

^aDepartment of Chemistry, Indian Institute of Technology Guwahati, Guwahati-781039. India.

^bCentre for Nanotechnology, Indian Institute of Technology Guwahati, Guwahati, 781039. India.

^cJyoti and Bhupat Mehta School of Health Science and Technology, Indian Institute of Technology Guwahati, Guwahati, 781039. India.

*Corresponding Author's email: pki@iitg.ac.in

Table of Contents

_Toc209993031

EXPERIMENTAL SECTION	4
Materials and methods:	4
Photoluminescence quantum yield (ϕ).	4
Limit of detection (LOD):	5
Cell Viability Assay:	5
Molecular docking:	5
Caution for handling of serum sample:	6
Serum Sample Analysis:	6
Figure S1: MALDI-TOF spectra for monomer M3	8
Figure S2: ^1H NMR of M3 in CDCl_3	8
Figure S3: ^{13}C NMR spectra of M3 in CDCl_3	8
Figure S4: MALDI-TOF spectra for monomer M4.	9
Figure S5: ^1H NMR of M4 in CDCl_3	10
Figure S6: ^{13}C NMR spectra of M4 in CDCl_3	10
Figure S7: ^1H NMR spectra of M5 in CDCl_3	11
Figure S8: ^{13}C NMR spectra of M5	12
Figure S9: ^1H NMR spectra of M6.	13
Figure S10: ^{13}C NMR spectra of M6 in CDCl_3	13
Table S1: The molar ratio of monomers used in polymerization of P1, P2 and P3 along with their yield (MW)	14
Figure S11: ^1H NMR spectra of P1 in CDCl_3	16
Figure S12: ^1H NMR spectra of P2 in CDCl_3	16
Figure S13: ^1H NMR spectra of P3 in CDCl_3	17
Figure S14: ^1H NMR spectra of PFAN in DMSO-d_6	18
Figure S15: Optimized structure of M4 monomer using B3LYP and 6-31G (d,p) of Gaussian software ³	18
Figure S16: TEM images and DLS measurement of M4 monomer	19
Figure S17: Schematic representation of polymers and the percentage contribution of monomers in the overall emission of polymers.	19

Figure S18: FESEM images of (a) P1, (b) P2, (c) P3 in 99 % f_w ; (d) solid state emission spectra and (e) their corresponding Quantum yield and photograph under UV lamp (365 nm).....	20
Figure S19: Solvent dependent study of PFAN.	20
Figure S20: (a) Viscosity and (b) temperature dependent study of PFAN.....	20
Figure S21: Selectivity study of PFAN with various (a) metal ions and (b) anions	21
Figure S22: The stability and repeatability of the PFAN polymer under various physiological conditions i.e. HEPES buffer pH 7.4 and temperature 37 °C.	21
Figure S23: Optimized structure of PFAN monomer using B3LYP function 631G (d, p, charge = +2) basis set of Gaussian Program 16.	21
Figure S24: Mechanism of BSA detection: (a) UV-Vis spectra of PFAN by addition of BSA; (b) DLS profile of PFAN, BSA and PFAN-BSA; (c) Zeta potential and (d) Lifetime decay profile of PFAN before and after addition of BSA; FESEM images of PFAN (e) before and (f) after addition of BSA.....	22
Table S2: Lifetime decay data for PFAN in absence and presence of HSA and BSA with an excitation pulse of 405 nm laser	22
Figure S25: PL spectra of P3 in absence and presence of 100 $\mu\text{g mL}^{-1}$ (a) HSA and (b) BSA.	23
Table S3: Isoelectric point (IP) ^{4,5} of various proteins and enzymes at pH 7.....	23
Figure S26: Binding site analysis of PFAN towards HSA using (a) ibuprofen, (b) phenyl butazone and (c) hemin.	23
Figure S27: Separation of serum from blood samples.	24
Table S4: Comparison of our sensing system with the clinical data.....	24
Figure S28: Photograph under UV lamp for (a) BSA (0- 90 $\mu\text{g mL}^{-1}$) detection by PFAN, (b) corresponding G/R value).	24
Table S5 Comparison table of HAS and BSA detection with the reported literature	25
REFERENCES	31

EXPERIMENTAL SECTION

Materials and methods:

The reagents 9,10 dibromoanthracene, 4 formyl phenyl boronic acid, 4 bromophenyl acetonitrile, were procured from TCI chemicals and bis-(pinacolato)diborane, dppf-1,1'-bis(diphenylphosphanyl)ferrocene, tetra butyl ammonium iodide (TBAI), 1,6-dibromohexane, 2, 7 dibromo fluorine, Tetrakis(triphenylphosphine)palladium(0) [$\text{Pd}(\text{PPh}_3)_4(0)$] catalyst were procured from Sigma-Aldrich. THF, DMSO and all the organic solvents used in the study are of HPLC grade and procured from Merck, Human serum albumin (HSA), Bovine serum albumin (BSA), Immunoglobulin and all the interfering analytes used in the selectivity study were purchased from Sigma-Aldrich. Milli-Q water has been used for the preparation of the stock solution for all the experiments.

Recording of ^1H NMR (500 MHz, 600 MHz) and ^{13}C NMR (125MHz, 150 MHz) spectra were performed on the Varian-AS600 NMR spectrometer. For recording UV-Visible absorption spectra and photoluminescence spectra, Cary 60 UV-Vis Spectrophotometer and Horiba Fluoromax-4 spectrofluorometers have been used with 1 ml quartz cuvettes (path length = 1 cm, slit = 3 nm). FESEM images were obtained from the Zeiss Sigma Field Emission Scanning Electron Microscope (FESEM). Lifetime and quantum measurement were done in Edinburgh FLS1000 Photoluminescence Spectrometer Dynamic light scattering and Zeta potential measurements were done DLS spectrometer Malvern Nano ZS90. DFT study is performed for monomer in Gaussian09 and for polymer Gaussian16. Docking study was done in AutoDockTools-1.5.7

Photoluminescence quantum yield (ϕ).

The absolute quantum yield for P1, P2, P3 and PFAN polymers were determined by using Edinburgh FLS 1000 instrument through integrated sphere technique.

Limit of detection (LOD):

The lowest LoD was determined by analyzing the fluorescence spectra of PFAN with varying concentrations of HSA (0-0.25 $\mu\text{g mL}^{-1}$) and BSA (0-0.25 $\mu\text{g mL}^{-1}$) in water medium. Using the standard formula, $\text{LoD}=3.3\sigma/k$, the lowest LoD was calculated from the calibration curve, where the symbols σ and k represent the standard deviation of the blank (only polymer before addition of analyte) and calibration plot's slope respectively.

Cell Viability Assay:

MTT assay was performed to evaluate the cytotoxicity of the polymer PFAN using HEK 293 cell. Cells were seeded into a 96-well plate at the density of 10,000 cells/well and incubated for 24 h. Cells were washed with 1X PBS and followed by the treatment of series of different concentration of polymer PFAN at 0, 10, 20, 30, 40, 50, 60, 50, 60, 70, 80, 90 and 100 $\mu\text{g/mL}$ for 24 h at 37 °C in incubator. Cells were washed with 1X PBS on incubation of 24 h. 10 μL of MTT of stock concentration 5 mg mL^{-1} and 90 μL DMEM medium was added to each well and incubated for 4 hours at 37 °C in incubator. After incubation for 4 h, 75 μL of medium was removed and 50 μL of DMSO was added to each well followed by further incubation of 10 minutes. The multimode microplate reader (Thermofisher Varioskan LUX) was used to record absorbance at wavelength of 490 nm. All the experiments were carried out in triplicate.

Molecular docking:

The purpose of molecular docking was to analyze the stable conformation of the probe while it is attached to a protein, focusing on its geometric and energetic properties. The software AutoDockTools-1.5.7 was utilized to produce a docked arrangement of PFAN monomer with HSA and BSA. This process involves the application of a genetic algorithm (GA) and a Lamarckian genetic algorithm to generate several conformations. The program was utilized to examine the binding free energies and binding locations of PFAN monomer within the active site of HSA/BSA. The crystal structure of HSA and BSA was obtained from RCSB PDB

(4K2C and 3V03) and underwent energy refinement, hydrogen additions, and solvent removal using AutoDockTools-1.5.7 to ensure that all residues achieved a proper and stable conformation. The Lamarckian GA (dpf file) was chosen as the output and utilized in AutoDockTools-1.5.7 to conduct docking simulations. The process of minimizing and optimizing the energy of PFAN monomer was also carried out. Ultimately, the analysis of the docking result of the PFAN monomer was conducted using Discovery Studio Visualizer programmes.¹ The docking structure with the lowest binding energy, as determined by AutoDockTools-1.5.7, was selected as the optimal binding conformation.

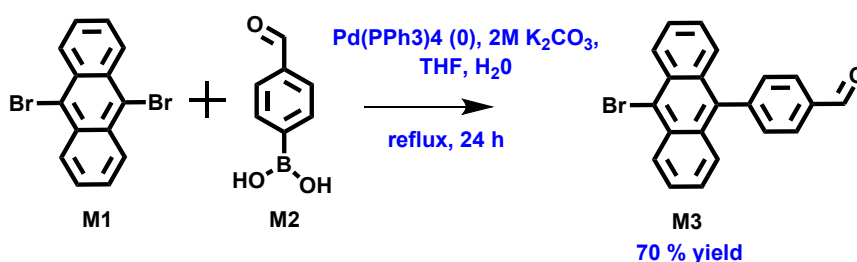
Caution for handling of serum sample:

Blood serum samples must be handled with care during the experiment. Human blood serum, particularly that of patients, can be highly dangerous if exposed; therefore, necessary precautions must be followed when handling them. The serum samples were kept in a freezer at -20 °C. To ensure safety, disposable gloves were worn during all fluorescence studies.

Serum Sample Analysis:

Fresh serum samples were collected from IIT G Hospital and diluted 100 times with Milli Q water to estimate HSA using the standard addition method. The serum samples were then spiked with 0 mg mL⁻¹, 0.5 mg mL⁻¹, 1.5 mg mL⁻¹, and 3.0 mg mL⁻¹ of HSA to make four distinct analytical samples. To record fluorescence spectra, 10 µl of each sample was introduced in a 1ml cuvette containing PFAN polymer. Each measurement was taken three times, and the amount of HSA was calculated using the Standard Recovery Technique.

4-(10-bromoanthracen-9-yl)benzaldehyde (M3):



The monomer (M3) was synthesized by Suzuki Coupling reaction. A mixture of monomers 9,10 dibromoanthracene (M1) (500 mg, 1.49 mmol) and 4 formyl phenyl boronic acid (M2) (268.4 mg, 1.79 mmol) were taken in a clean RB flask fitted with water condenser and then made the system inert by degassing followed by purging with argon gas. Thereafter, 5mg of catalyst Pd(PPh₃)₄ (0) were added maintaining the inert condition. A mixture of THF (9 ml) and 2M K₂CO₃ (3 ml) were injected into the reaction mixture and were made inert by applying free-thaw degassing technique (3 times). The reaction mixture was stirred at reflux condition under an argon atmosphere and the progress of reaction were monitored by TLC. After 24 h., the reaction was stopped and extracted with CHCl₃/water. The organic layer was dried under vacuum and it was purified by column chromatography by 30 % CHCl₃/hexane solvent fraction. (yellow color solid, Yield = 70 %, 430 mg).

MALDI_TOF: The mass of monomer M3 (m/z = 360.988)

¹H NMR (500 MHz, CDCl₃, δ (ppm): 10.20 (s, 1H), 8.64 (d, J = 8.9 Hz, 2H), 8.12 (d, J = 8.0 Hz, 2H), 7.61 (t, J = 6.4 Hz, 4H), 7.55 (d, J = 8.8 Hz, 2H), 7.40 (dd, J = 8.0, 6.9 Hz, 2H).

¹³C NMR (150 MHz, CDCl₃, δ (ppm): 191.95, 145.29, 135.95, 135.86, 132.02, 130.02, 130.57, 130.19, 129.85, 128.09, 127.10, 126.72, 126.08, 123.64.

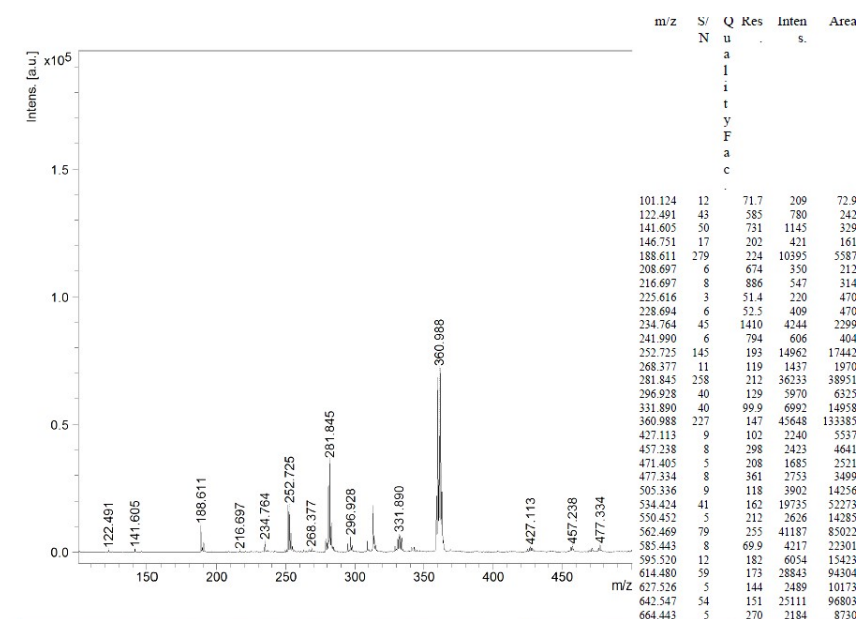


Figure S1: MALDI-TOF spectra for monomer M3

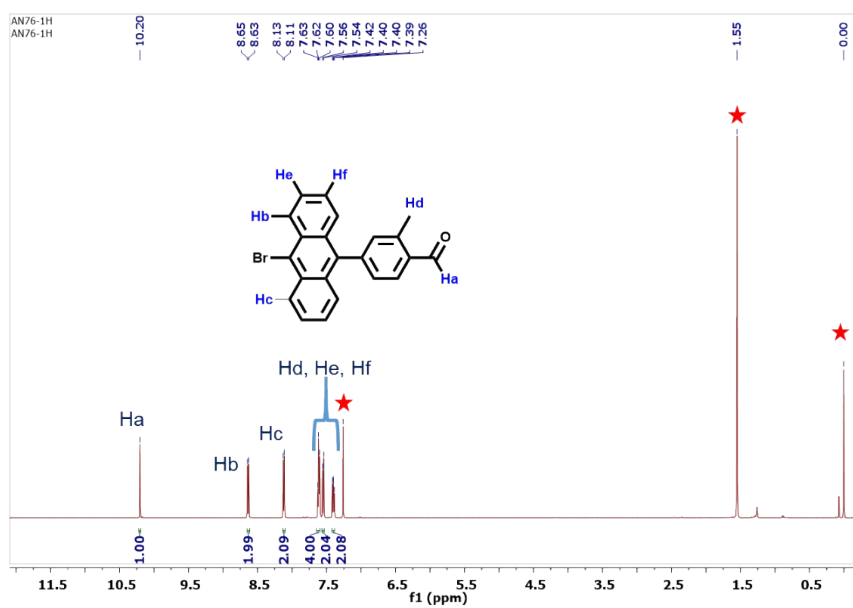


Figure S2: ^1H NMR of M3 in CDCl_3

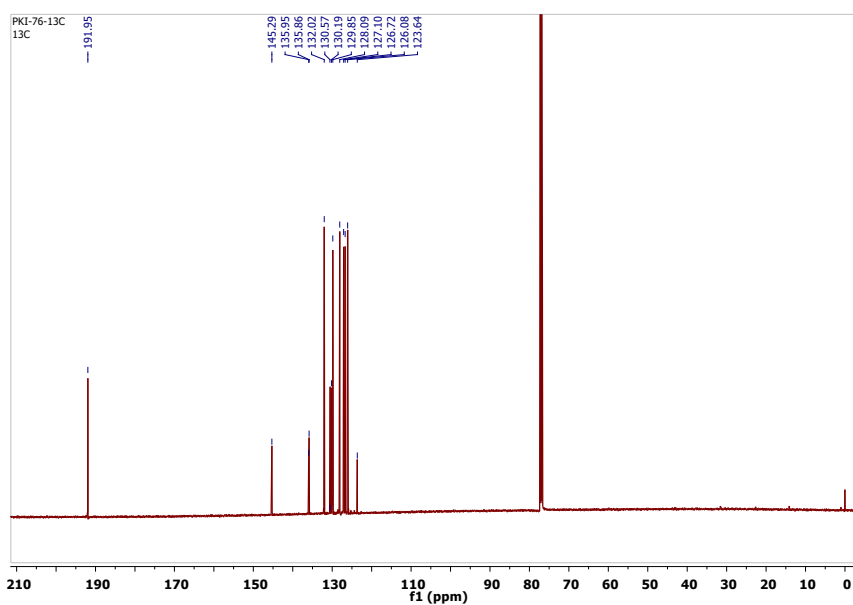
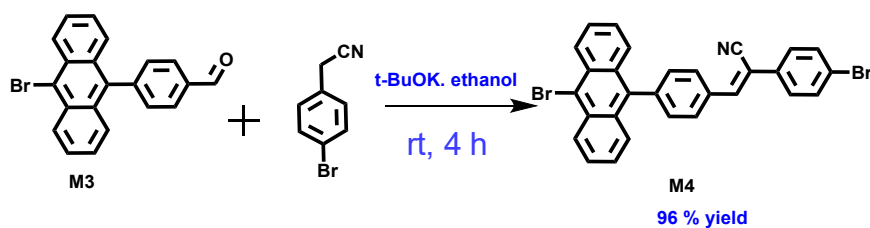


Figure S3: ^{13}C NMR spectra of M3 in CDCl_3

(Z)-3-(4-(10-bromoanthracen-9-yl)phenyl)-2-(4-bromophenyl)acrylonitrile (M4):



The monomer M4 was synthesized by Knoevenagel Condensation reaction. The monomer M3 (50 mg, 0.138 mmol) and 4 bromophenyl acetonitrile were solubilised in 20 ml ethanol at 50 °C with continuous stirring. 23 mg of Potassium tertiary butoxide (t-BuOK) was solubilised in 2 ml ethanol and then injected into the reaction mixture dropwise. After the product gets precipitated as yellowish precipitate from the reaction mixture. The progress of the reaction was monitored by TLC and after 4 h the precipitate was filtered through Whatman filter paper and then wash repeatedly by ethanol to get the pure amorphous yellow ppt. (yield= 96 %, 72 mg).

MALDI_TOF: The mass of monomer M4 ($m/z = 538.909$)

^1H NMR (600 MHz, CDCl_3 , δ (ppm): 8.63 (s, 2H), 8.12 (d, $J = 8.0$ Hz, 2H), 7.69 (s, 1H), 7.64 (d, $J = 8.4$ Hz, 6H), 7.61 (d, $J = 7.9$ Hz, 2H), 7.54 (d, $J = 8.1$ Hz, 2H), 7.43 – 7.40 (m, 2H).

^{13}C NMR (150 MHz, CDCl_3 , δ (ppm): 142.24, 141.39, 132.98, 130.22, 129.44, 128.08, 127.56, 127.07, 126.94, 125.95, 123.66, 117.68, 111.04

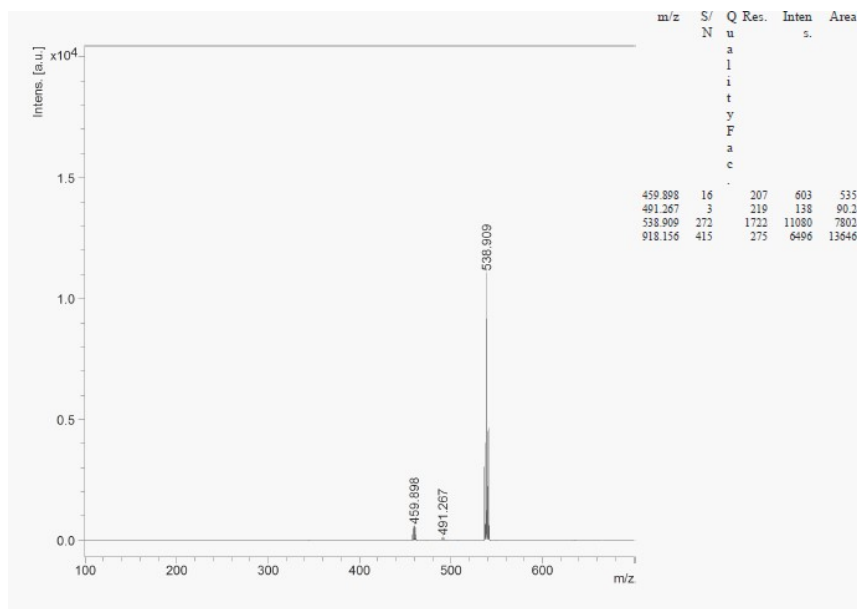


Figure S4: MALDI-TOF spectra for monomer M4.

The synthesis of the monomers M5 was done by following the already reported procedures.² The starting material 2, 7 dibromo fluorene (1g, 3.106 mmol), and tetra butyl ammonium iodide (TBAI) (0.229 g, 0.621 mmol) were taken in a clean RB flask and made inert condition by applying free-thaw and degassing technique (3 times). After that, 1,6-dibromohexane (2.82 mL, 18.636 mmol) followed by 50 % NaOH were injected cautiously through a syringe, maintaining the inert condition. Finally, the reaction was performed at 80 °C with proper stirring for 5 h. TLC in hexane was used to monitor reaction completion, then separated the organic part from water in a separating funnel with water/chloroform mixture. The excess 1,6-dibromohexane from the recovered organic layer dried by Kugelrohr and further purification was done by column chromatography with hexane as eluent to obtain the final product as white crystalline solid. (Yield = 95 %, 1.92 g)

¹H NMR (600 MHz, CDCl₃, δ(ppm): 7.52-7.54(d, 2H), 7.43-7.48 (m, 4H), 3.28-3.31 (t, 4H), 1.90-1.95 (p, 4H), 1.64-1.71(p, 4H), 1.17-1.24(p, 4H), 1.05-1.12(p, 4H), 0.56-0.63(4H).

¹³C NMR (150 MHz, CDCl₃, δ (ppm): 152.19, 139.09, 130.05, 126.12, 121.58, 121.53, 55.57, 40.03, 32.79, 32.61, 28.95, 27.75, 23.47.

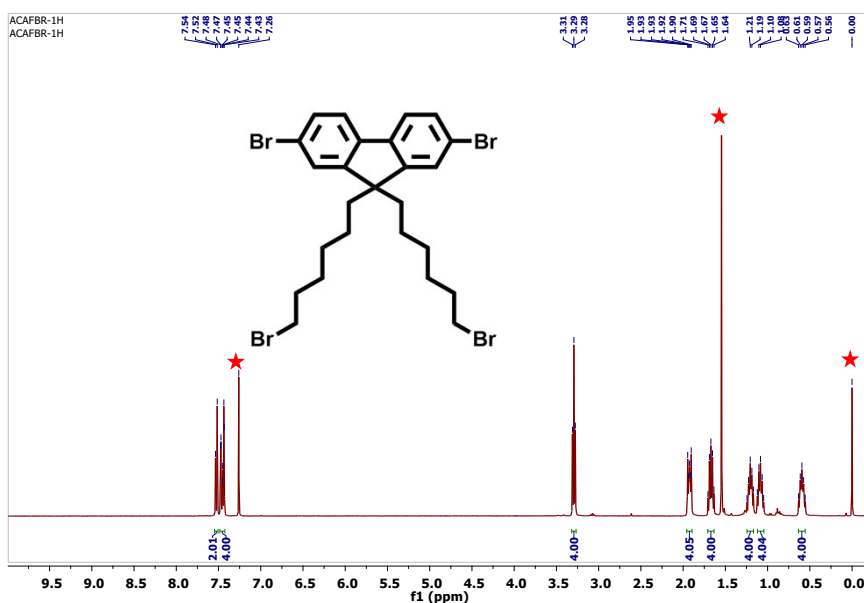


Figure S7: ¹H NMR spectra of M5 in CDCl₃.

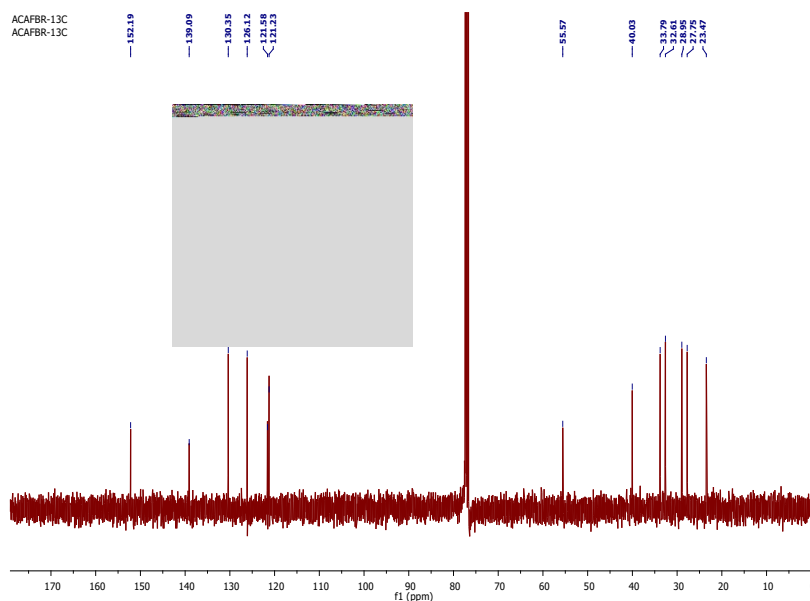
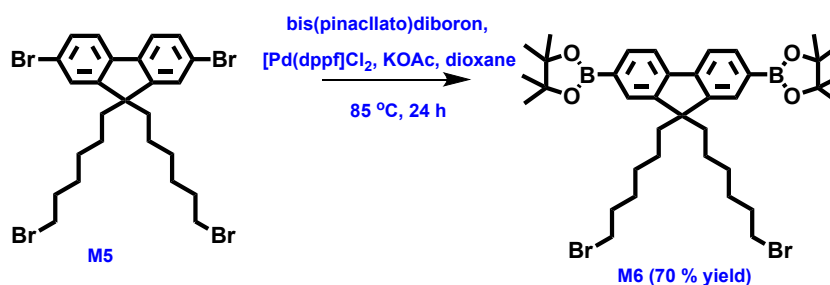


Figure S8: ^{13}C NMR spectra of M5

2,7-bis[9,9'-bis(6''-bromohexyl)fluorenyl]-4,4,5,5-tetramethyl[1,3,2]dioxaborolane (M6):



The mixture monomer M5 (1g, 1.5 mmol), bis-(pinacolato)diborane (0.95 g, 3.75 mmol) and KOAc (1g, 10 mmol) were taken in a clean 250 ml RB flask. The mixture is degassed and then 5mg of $[\text{Pd}(\text{dppf})\text{Cl}_2]$ (dppf-1,1'-bis(diphenylphosphanyl)ferrocene) was added cautiously followed by 12 ml 1,4 dioxane (dry). The reaction stirred properly at 85°C for 24 h. Then the mixture was dried at high vacuum and then extracted the organic soluble part by using ethyl acetate/ water mixture. Further purification was done by flash chromatography using 5 % ethyl acetate hexane mixture as eluent to get M6 as white crystals (0.63 g, 66 %)

^1H NMR (600 MHz, CDCl_3 , $\delta(\text{ppm})$): 7.73-7.75(d, 2H), 7.65-7.66 (m, 4H), 3.23-3.27 (t, 4H), 1.98-2.05 (p, 4H), 1.57-1.67 (p, 4H), 1.39 (s, 24H), 1.11-1.16(p, 4H), 1.00-1.07 (p, 4H), 0.50-0.57(4H).

^{13}C NMR (150 MHz, CDCl_3 , δ (ppm): 150.17, 143.50, 133.90, 129.12, 119.94, 83.56, 55.13, 40.17, 34.06, 32.49, 29.32, 27.38, 24.50, 23.57

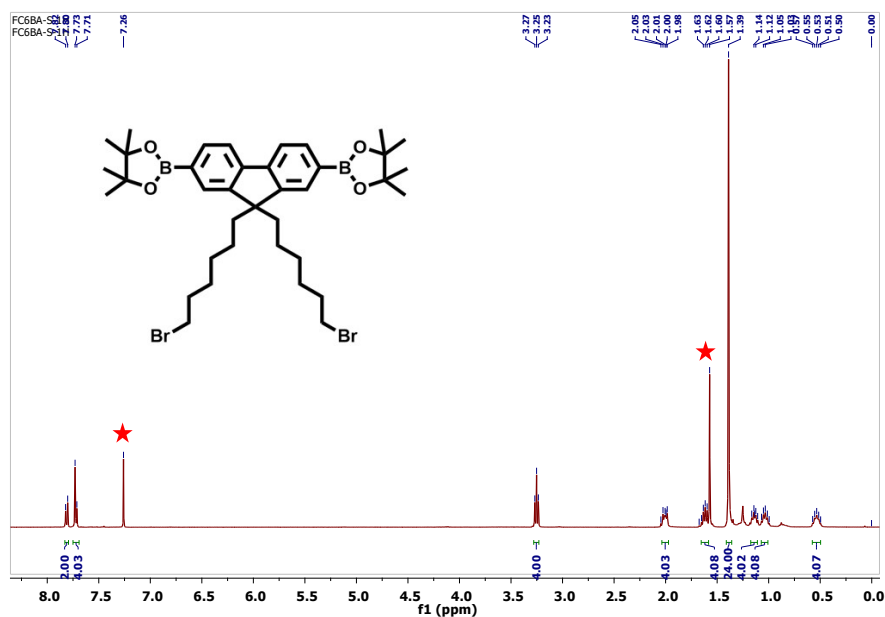


Figure S9: ^1H NMR spectra of M6.

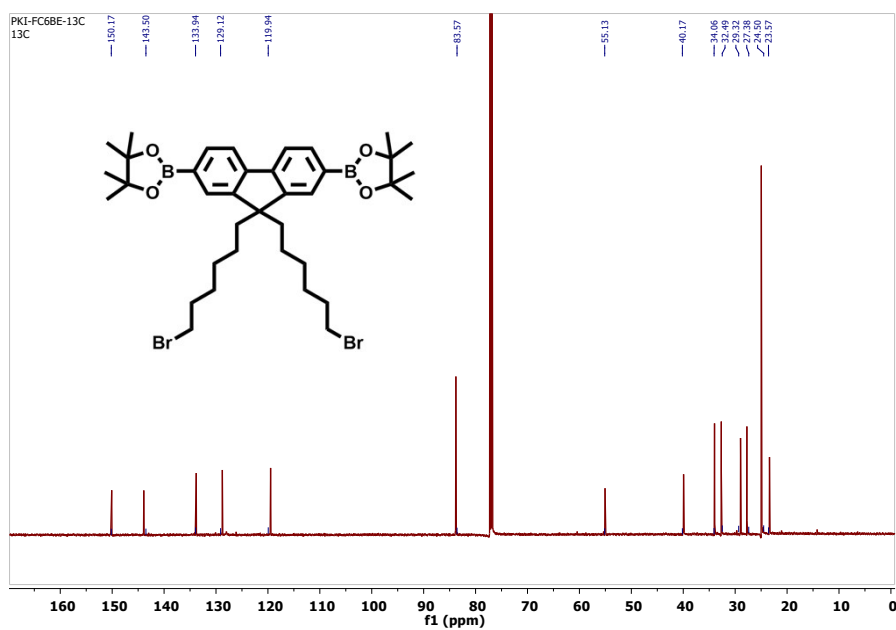


Figure S10: ^{13}C NMR spectra of M6 in CDCl_3 .

Synthesis of P1, P2 and P3 polymers:

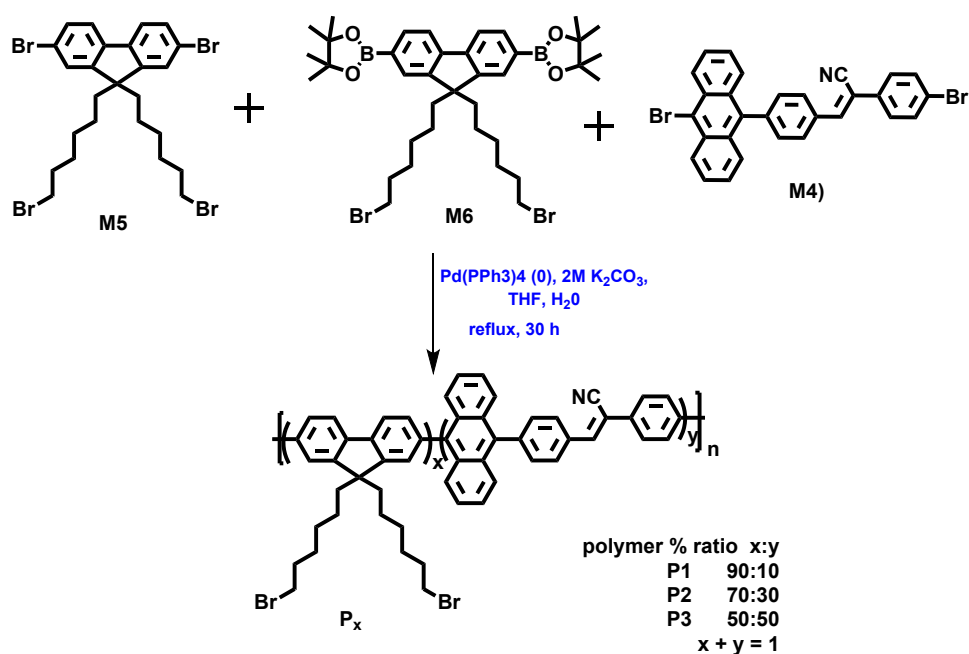


Table S1: The molar ratio of monomers used in polymerization of P1, P2 and P3 along with their yield (MW)

Polymer	Mole fractions of monomers taken			Yield (%)	MW (gmole ⁻¹)	PDI
	M4	M5	M6			
	MW	MW	MW			
	539.27	650.13	744.26			
	gmole ⁻¹	gmole ⁻¹	gmole ⁻¹			
P1	43.47 mg (0.08mmoles)	210 mg (0.322mmoles)	300 mg (0.403mmoles)	470 mg (85 %)	16688	1.60
P2	130.39 mg (0.242 mmole)	104.8 mg (0.161mmoles)	300 mg (0.403mmoles)	430 mg (80 %)	14391	1.54
P3	217.37 mg (0.403 mmoles)	0	300 mg (0.403mmoles)	450 mg (87 %)	15324	1.78

They were synthesized by Suzuki Coupling reaction by taking the required molar ratio of monomers M4, M5 and M6 as given in Table S1. A mixture of monomers M4, M5 and M6 were taken in a clean RB flask fitted with a condenser and then made the system inert by degassing followed by purging with argon gas. Thereafter, 5 mg of catalyst $\text{Pd(PPh}_3)_4$ (0) were added maintaining the inert condition. A mixture of THF (9 mL) and 2M K_2CO_3 (3mL) were injected into the reaction mixture and were made inert by applying freeze-thaw degassing technique (3 times). The reaction mixture was stirred at reflux condition under an argon atmosphere. After 30 h., the reaction was cooled down and extracted with CHCl_3 /water. The organic layer was dried under vacuum and purified by repeated precipitation in methanol and acetone. The molecular weight (MW) of polymers were determined by GPC using polystyrene as a standard.

For P1:

^1H NMR (600 MHz, CDCl_3 , δ (ppm): 7.87 (b), 7.73-7.69 (b), 7.60-7.51 (b), 7.12-6.91 (b) 3.0 (b), 2.19 (b) 1.28-1.19 (b), 1.70 (b) 0.84 (b).

For P2:

^1H NMR (600 MHz, CDCl_3 , δ (ppm): 8.11-7.95 (b), 7.75-7.57 (b), 7.37-7.31 (b), 7.06 (b), 7.84 (b), 3.22 (b), 2.05 (b) 1.62 (b), 1.09 (b) 0.76 (b).

For P3:

^1H NMR (600 MHz, CDCl_3 , δ (ppm): 8.17-8.01 (b), 7.82-7.77 (b), 7.62 (b), 7.49 (b), 7.36 (b), 3.25 (b), 1.98 (b) 1.67 (b), 1.09 (b) 0.82-0.67 (b).

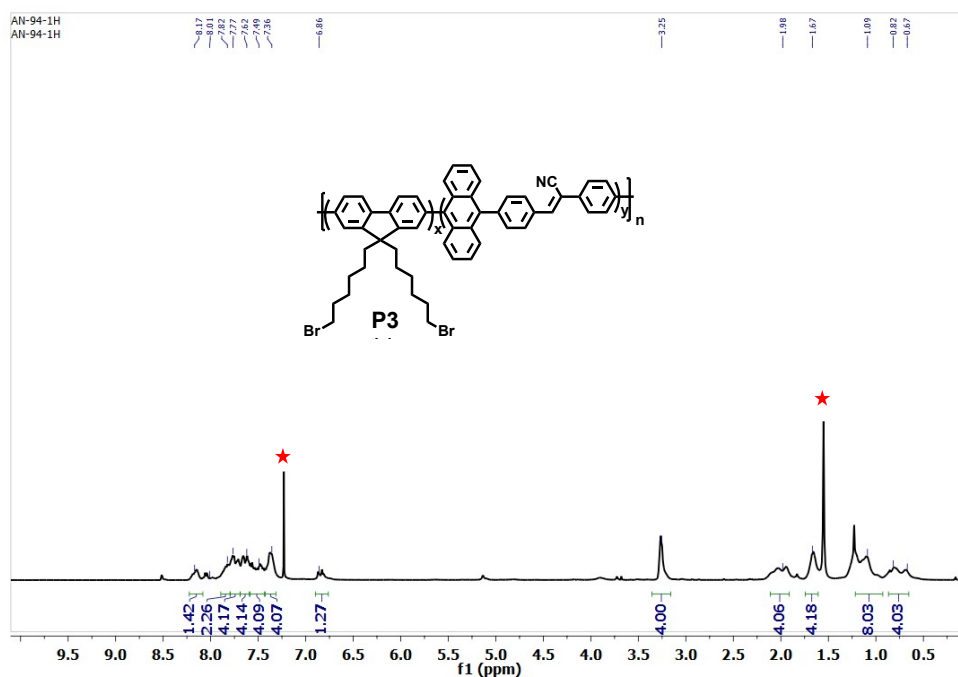


Figure S13: ^1H NMR spectra of P3 in CDCl_3 .

(Z)-3,3'-((2-(10-(4-(2-cyano-2-(p-tolyl)vinyl)phenyl)anthracen-9-yl)-7-methyl-9H-fluorene-9,9-diyl)bis(hexane-6,1-diyl))bis(1-methyl-1H-imidazol-3-ium) (PFAN) :



The final polymer PFAN was synthesized by vigorous stirring of P3 (100 mg), 1-methyl imidazolium (1.5 ml) and K_2CO_3 (100 mg) in 2 mL of dry DMF for 24 h at 110 °C. After the completion of the reaction, DMF and excess 1-methyl imidazolium were removed by precipitation in diethyl ether. Then further reprecipitated from acetone followed by washing with THF. Finally, the precipitate was dried under vacuum to achieve the desired brownish-yellow polymer (PFAN). (Yield = 80 %, 80 mg)

^1H NMR (400 MHz, CDCl_3 , δ (ppm)): 8.99-9.03 (b), 8.28(b), 7.99 (b), 7.63-7.65 (b), 7.36-7.48(b), 3.77-4.01 (b), 2.47 (b), 1.56-1.58 (b), 1.04 (b), 0.58 (b)

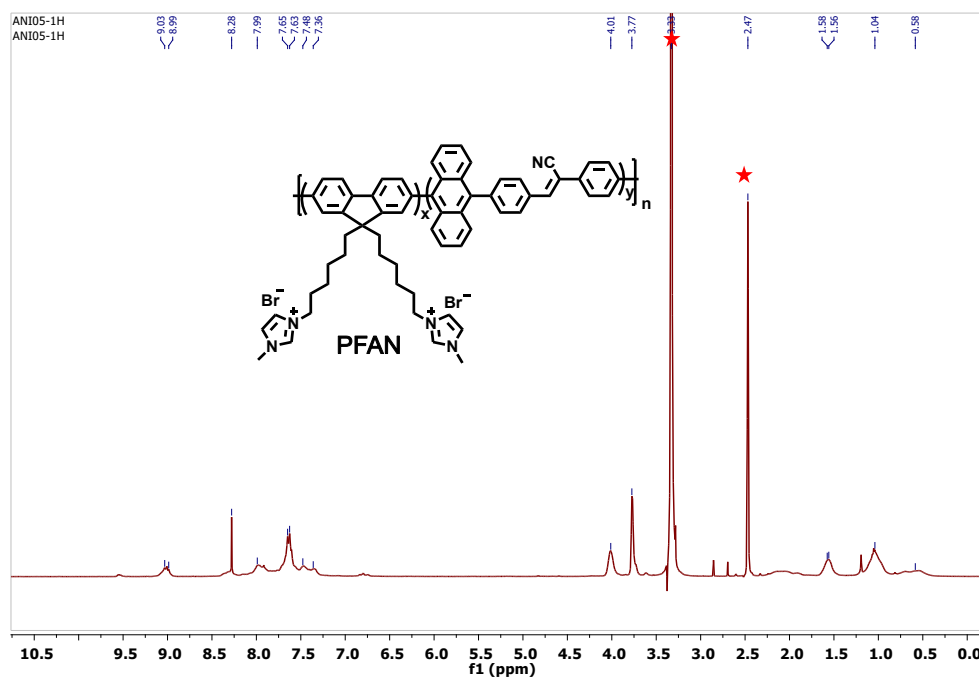


Figure S14: ^1H NMR spectra of PFAN in DMSO-d_6 .

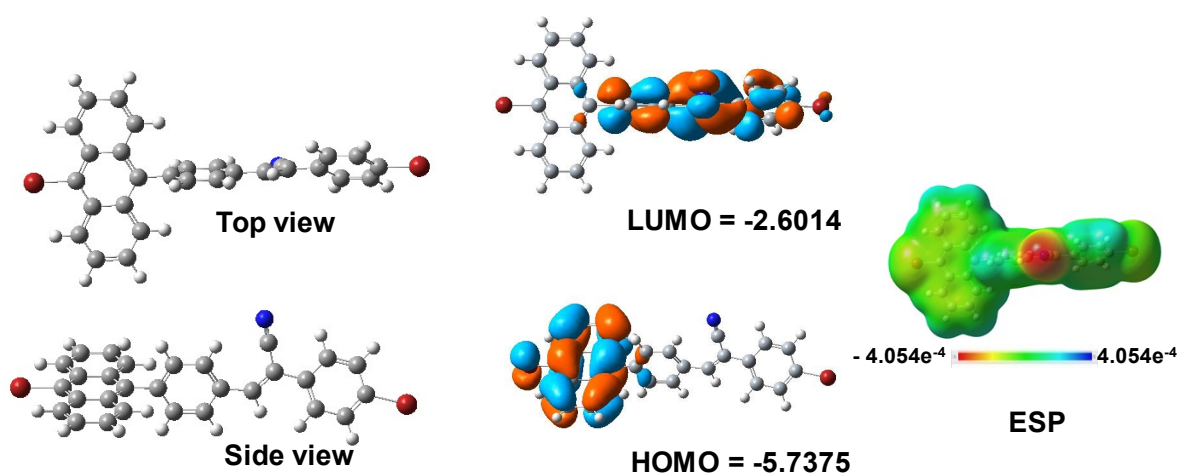


Figure S15: Optimized structure of M4 monomer using B3LYP and 6-31G (d,p) of Gaussian software.³

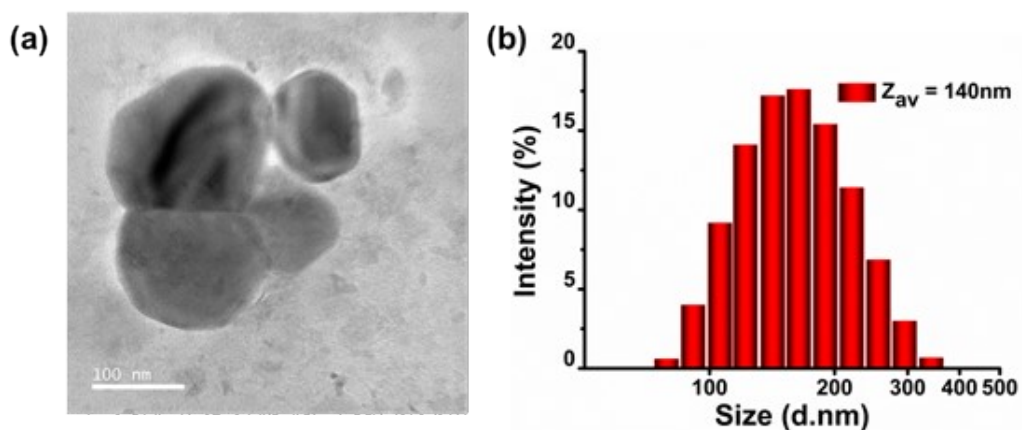


Figure S16: (a) TEM images and (b) DLS measurement of M4 monomer.

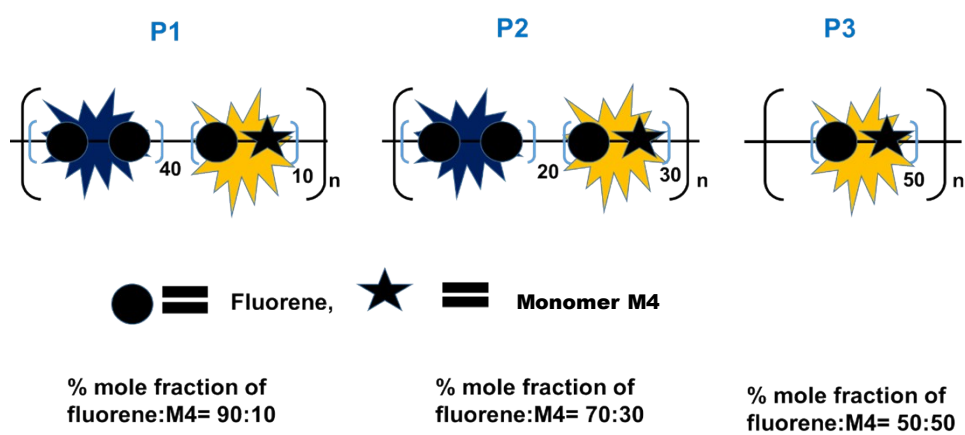


Figure S17: Schematic representation of polymers and the percentage contribution of monomers in the overall emission of polymers.

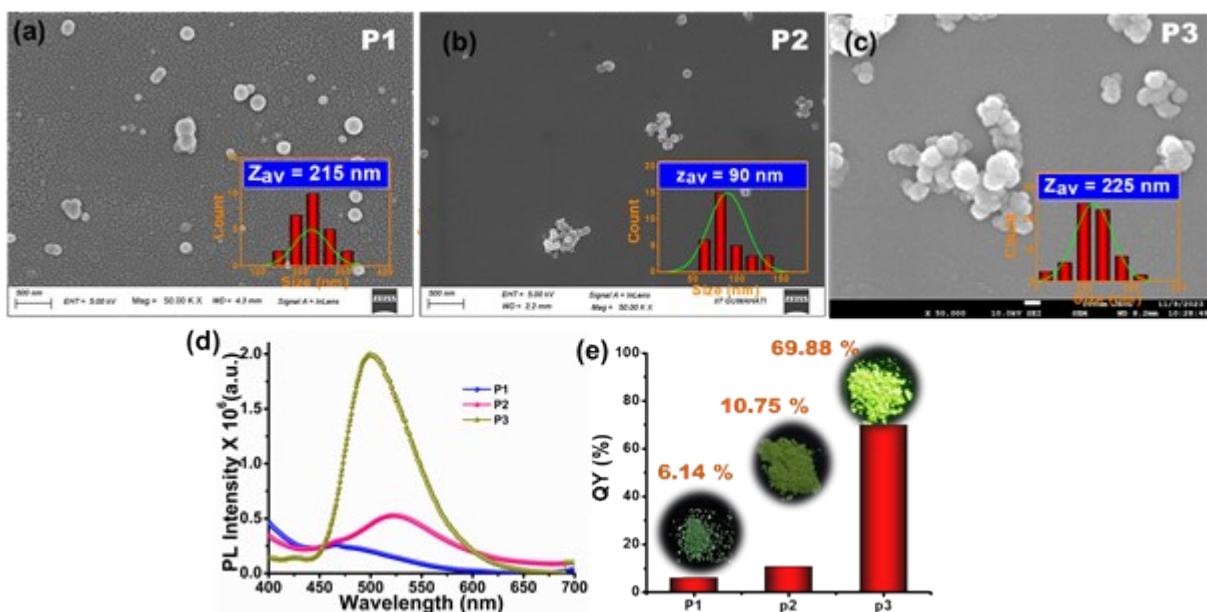


Figure S18: FESEM images of (a) P1, (b) P2, (c) P3 in 99 % f_w ; (d) solid state emission spectra and (e) their corresponding Quantum yield and photograph under UV lamp (365 nm).

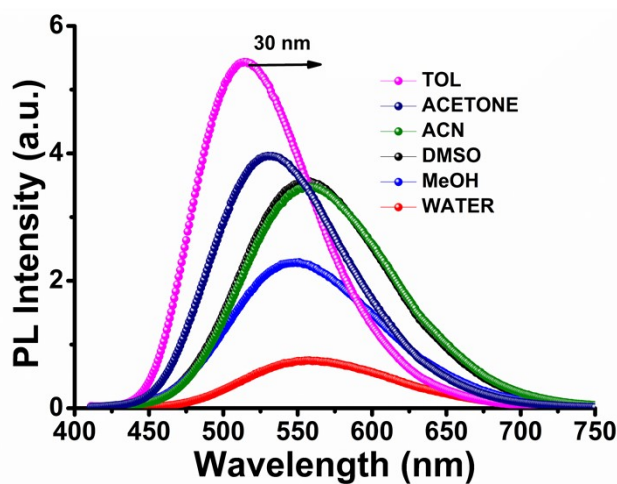


Figure S19: Solvent dependent study of PFAN.

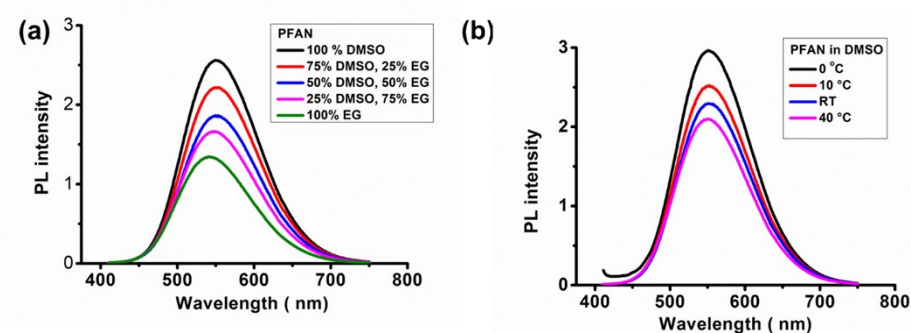


Figure S20: (a) Viscosity and (b) temperature dependent study of PFAN.

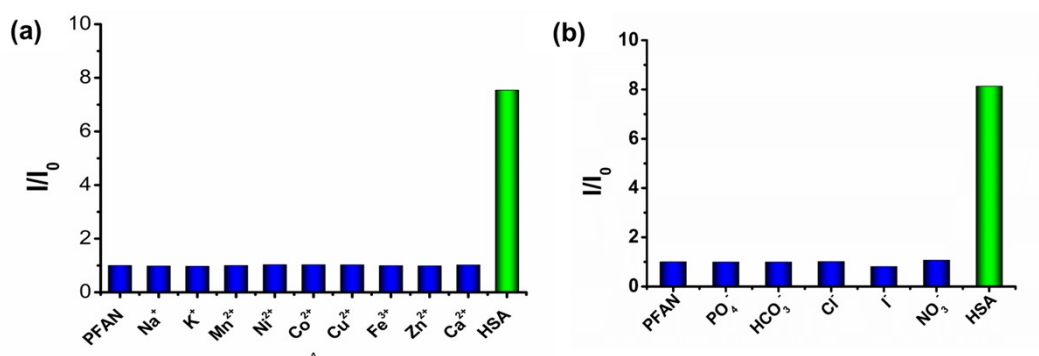


Figure S21: Selectivity study of PFAN with various (a) metal ions and (b) anions

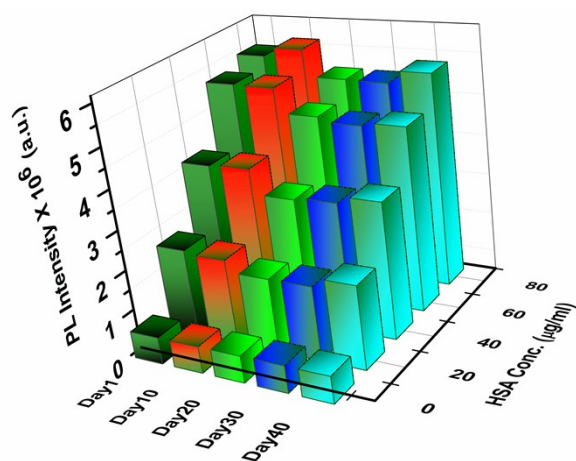


Figure S22: The stability and repeatability of the PFAN polymer under various physiological conditions i.e. HEPES buffer pH 7.4 and temperature 37 °C.

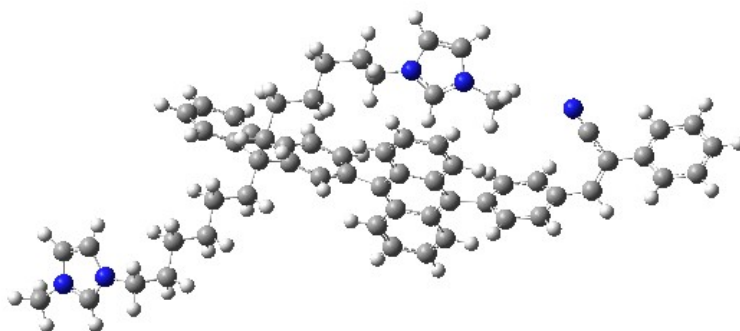


Figure S23: Optimized structure of PFAN monomer using B3LYP function 631G (d, p, charge = +2) basis set of Gaussian Program 16.

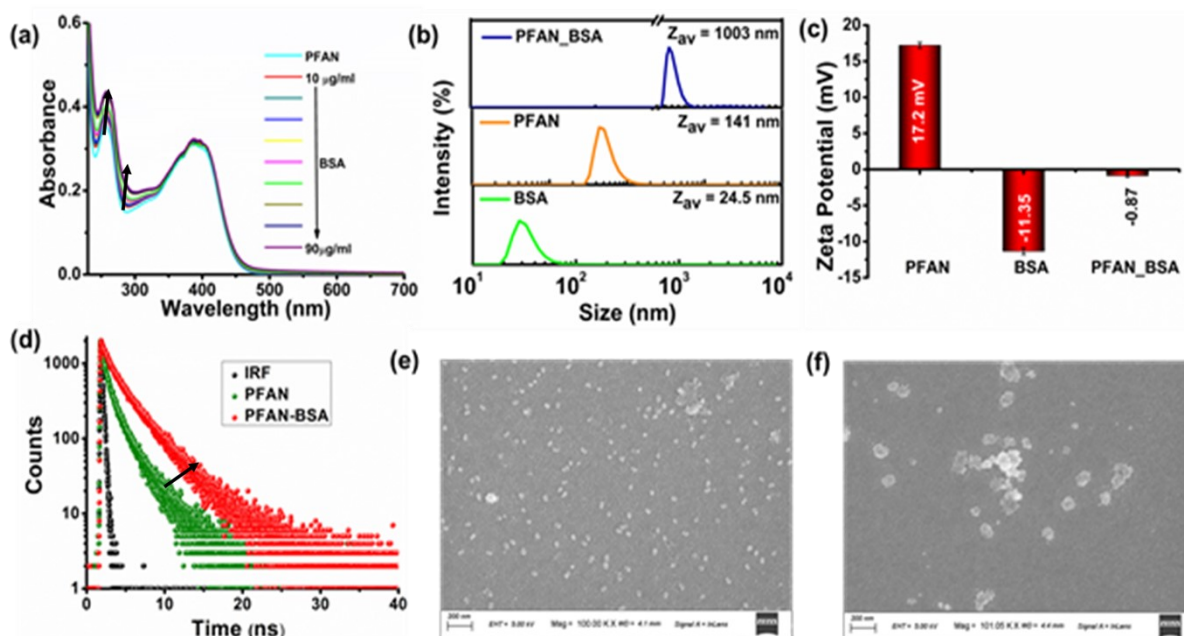


Figure S24: Mechanism of BSA detection: (a) UV-Vis spectra of PFAN by addition of BSA; (b) DLS profile of PFAN, BSA and PFAN-BSA; (c) Zeta potential and (d) Lifetime decay profile of PFAN before and after addition of BSA; FESEM images of PFAN (e) before and (f) after addition of BSA.

Table S2: Lifetime decay data for PFAN in absence and presence of HSA and BSA with an excitation pulse of 405 nm laser

Sample	a_1 (%)	τ_1 (ns)	a_2 (%)	τ_2 (ns)	χ^2	τ_{av} (ns)
PFAN	58.714	0.591	41.286	2.504	1.047	1.38
PFAN-HSA	45.331	1.260	54.669	3.799	1.046	2.65
PFAN-BSA	43.991	1.177	56.009	3.691	1.030	2.58

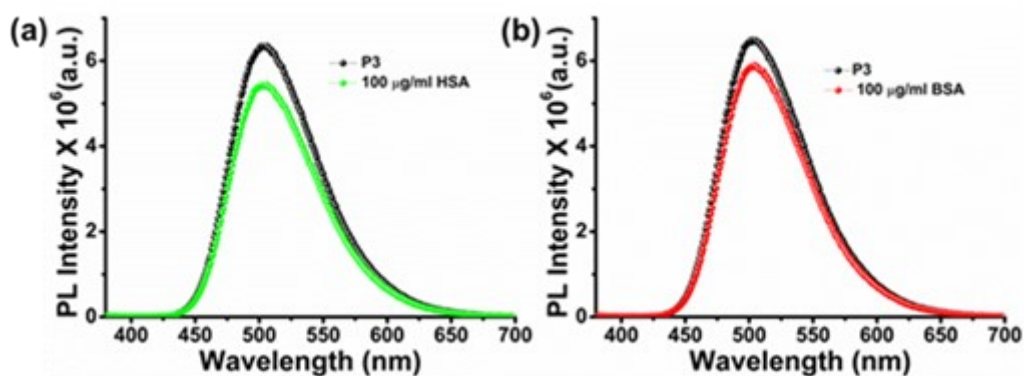


Figure S25: PL spectra of P3 in absence and presence of 100 $\mu\text{g mL}^{-1}$ (a) HSA and (b) BSA.

Table S3: Isoelectric point (IP)^{4,5} of various proteins and enzymes at pH 7

Proteins	IP (net charge at pH 7)
Cytc	10.5(+)
HRP	9.0(+)
trypsin	10.5(+)
RNase	9.6(+)
pepsin	2.5(−)
Hb	6.8(−)
BSA	4.8(−)
HSA	5.2(−)

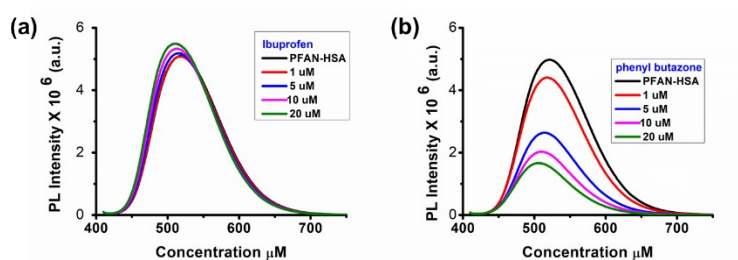


Figure S26: Binding site analysis of PFAN towards HSA using (a) ibuprofen and (b) phenyl butazone

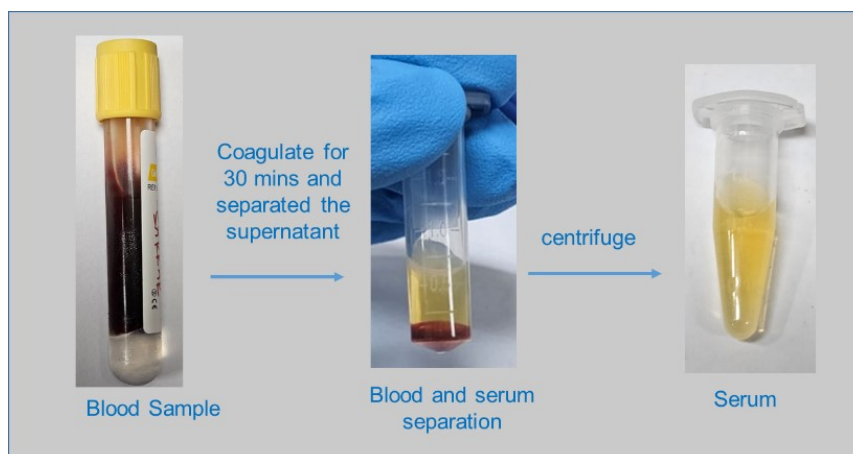


Figure S27: Separation of serum from blood samples.

Table S4: Comparison of our sensing system with the clinical data

Sl no.	Age (years)	HSA detected by our method (g dL ⁻¹)	HSA detected by clinical method (g dL ⁻¹)
1	71	3.87±2.13	4.0
2	94	3.93 ± 1.52	3.6
3	72	3.25 ± 2.56	3.4

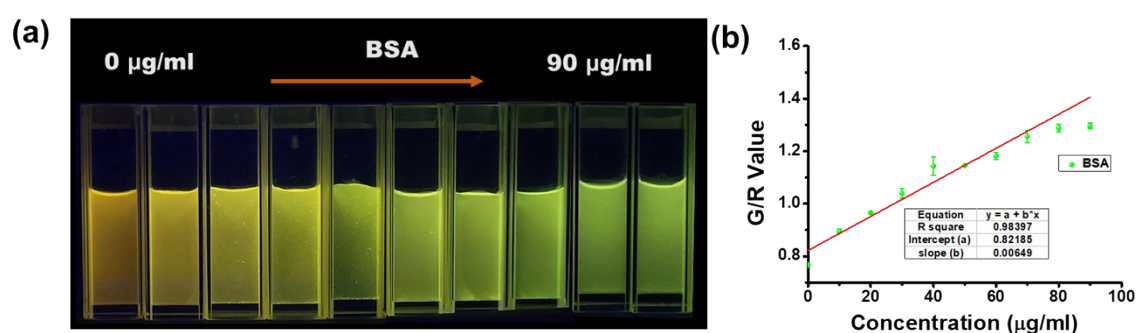


Figure S28: Photograph under UV lamp for (a) BSA (0- 90 µg mL⁻¹) detection by PFAN, (b) corresponding G/R value).

Table S5 Comparison table of HAS and BSA detection with the reported literature

Publication s	Material used	Limit of detectio n (LOD)	Selectivi ty	Technique	Mechani sm	PoC Testi ng
Present work	AIEE conjugated polyelectrolytes (PFAN)	BSA- 106.7 ng/mL HSA- 50 ng/mL	Selective	Fluorescence	Molecular binding induced AIEE	Yes
<i>Anal.Chem.</i> 2022, 94 ,10685–1 0694	Conjugated polymer surfactant ensembles	BSA 0.50 μg/mL HSA 0.81μg/ mL	Selective	Fluorescence	Intermolecular Reverse FRET	Yes
<i>Angew. Chem. Int. Ed.</i> 2020, 59 , 3131	hydroxychalcone derivative	HSA 1.08 μg/ml	Selective	Fluorescence	De-aggregation	Yes
<i>Chem. Commun.</i> 2019, 55 , 13983	Flavanoid derivative	HSA 2.13 μg/mL	Selective	Fluorescence	AIE	No
<i>Chem. Commun.</i>	Styryl derivative	BSA 3.19	Selective	Fluorescence	TICT Inhibition	No

2018, 54 , 8383		µg/mL			n	
<i>Chem.</i>	2	SA 2.5	Selective	Fluorescence	AIE	No
<i>Commun.</i>	Dicyanomethyle	µg/mL				
2018, 54 , 8383	ne-3 cyano- 4,5,5-trimethyl- 2,5- dihydrofuran derivative					
<i>ACS Appl.</i>	Conjugated	Not	Not	Fluorecence	Metal	No
<i>Mater.</i>	polyelectrolyte-	Reported	Selective		Displace	
<i>Interfaces</i>	Pt(II) complex				ment	
2017, 9 , 33461						
<i>Anal. Chem.</i>	Small organic	HSA	Selective	Fluorecence	Disassem	No
2017, 89 , 10085	nanoprobe	0.14 µM (9.3 mg L ⁻¹)			bly Induced Emission	
<i>ACS Appl.</i>	Pentaaryl	BSA	Selective	Fluorecence	AIE	No
<i>Mater.</i>	substituted	2.18				
<i>Interfaces</i>	pyrrole	µg/mL				
2015, 7 , 26094		HAS 1.68 µg/mL				
<i>Macromolec</i>	Conjugated	Not	Not	Fluorescence	Charge	No

<i>ules</i>	polyelectrolytes	Reported	Selective		Transfer	
2009, 42 ,						
5933						
<i>Macromolec</i>	Conjugated	Not	Selective	Fluorescence	Interchai	No
<i>ules</i>	polyelectrolyte	Reported			n	
2008, 41 ,					FRET	
4003						
<i>Langmuir</i>	Conjugated	Not	Not	Fluorescence	Aggregat	No
2005,	polyelectrolyte	Reported	Selective		ion	
21 , 7985						
<i>Biochip J.</i>	Antibody-	Not	Selective	Electrical	chemical	No
2017, 11 ,	modified CNT-	reported		conductance	gating	
116–120.	FET				effects	
					from	
					HSA	
					bound to	
					mAHSA	
<i>Top. Catal.</i>	Thin Film of	10.3 μ M	Selective	Cyclic	Enhance	No
2025, 68 ,	Polydopamine/T	(HSA)		voltammetry	d	
677–686	iO2				electron	
	Nanoparticles				transfer	
					via	
					surface	
					modificat	
					ion and	

					complexa tion	
<i>Anal.</i>	MIP	5.3	Selective	Quartz	QCMs	No
<i>Bioanal.</i>	nanoparticles	µg/mL		crystal	devices	
<i>Chem.</i> 2024,	resulting from	(HSA)		microbalance	resonanc	
414 , 731–	solid-phase			(QCM)	e	
741	synthesis			sensor	frequenc	
					y	
					changes	
					when	
					mass	
					deposits	
					on the	
					electrode	
					surface	
<i>Nat.</i>	synthesized a	3 mg/L	Selective	Fluorescence	The	No
<i>Commun.</i> ,	suite of	(Albumi			nanotube	
2019, 10 ,	polycarbodiimid	n)			emission	
3605	e polymers to				response	
	concomitantly				behavior,	
	encapsulate				upon	
	carbon				interactio	
	nanotubes and				n	
	interact with				with	
	specific features				albumin,	

	of albumin				hypsochr omic emission response is caused by the known solvatoch romic behavior of nanotube .	
<i>J Clin Pathol.</i> 1987, 40 , 465-468	immunoturbidi metric method	2.5 mg/L (Albumi n)	-	Albumin measured in all samples by automated immunoturbi dimetry	-	No
<i>Microchim. Acta.</i> 2020, 187 , 208	absorbance nanoprobe based on the NCur-VO2+	11nM (Albumi n)	Selective	Absorbance	Determin ation of HSA via aggregati	No

	ensemble was				on of the	
	fabricated				NCur by	
					VO ₂ ⁺	
					and	
					subseque	
					ntly,	
					deaggreg	
					ation of	
					the	
					NCur-	
					VO ₂ ⁺	
					ensemble	
					in the	
					presence	
					of HSA	
<i>Anal.</i>	Self-Assembled	0.5	Not	SERS	Electrost	NO
<i>Chem.</i> 2010,	Protein-Silver	µg/mL	Selective		atic	
82 , 7596–	Nanoparticle	(BSA)			interactio	
7602					n with	
					isoelectric	
					point and	
					size is	
					the	
					important	
					parmeter.	

REFERENCES

- 1 M. F. Sanner, *J Mol Graph Model*, 1999, **17**, 57–61.
- 2 G. Saikia and P. K. Iyer, *J. Org. Chem*, 2010, **75**, 2714–2717.
- 3 M. J. Frisch, G. W. Trucks, H. B. Schlegel, G. E. Scuseria, M. A. Robb, J. R. Cheeseman, G. Scalmani, V. Barone, B. Mennucci, G. A. Petersson, H. Nakatsuji, M. Caricato, X. Li, H. P. Hratchian, A. F. Izmaylov, J. Bloino, G. Zheng, J. L. Sonnenberg, M. Hada, M. Ehara, K. Toyota, R. Fukuda, J. Hasegawa, M. Ishida, T. Nakajima, Y. Honda, O. Kitao, H. Nakai, T. Vreven, J. A. Montgomery, J. E. Peralta, F. Ogliaro, M. Bearpark, J. J. Heyd, E. Brothers, K. N. Kudin, V. N. Staroverov, R. Kobayashi, J. Normand, K. Raghavachari, A. Rendell, J. C. Burant, S. S. Iyengar, J. Tomasi, M. Cossi, N. Rega, J. M. Millam, M. Klene, J. E. Knox, J. B. Cross, V. Bakken, C. Adamo, J. Jaramillo, R. Gomperts, R. E. Stratmann, O. Yazyev, A. J. Austin, R. Cammi, C. Pomelli, J. W. Ochterski, R. L. Martin, K. Morokuma, V. G. Zakrzewski, G. A. Voth, P. Salvador, J. J. Dannenberg, S. Dapprich, A. D. Daniels, Ö. Farkas, J. B. Foresman, J. V. Ortiz, J. Cioslowski and D. J. Fox, *Gaussian 09*, Revision B.01; Gaussian Inc.: Wallingford, CT, 2010.
- 4 S. Hussain, X. Chen, C. Wang, Y. Hao, X. Tian, Y. He, J. Li, M. Shahid, P. K. Iyer and R. Gao, *Anal. Chem*, 2022, **94**, 10685–10694.
- 5 P. Sun, X. Lu, Q. Fan, Z. Zhang, W. Song, B. Li, L. Huang, J. Peng and W. Huang, *Macromolecules*, 2011, **44**, 8763–8770.